Simultaneous Stripping Detection of Pb(II), Cd(II) and Zn(II) Using a Bimetallic Hg-Bi/Single-Walled Carbon Nanotubes Composite Electrode

Ruizhuo Ouyang, **Zhenqian Zhu**, **Clarissa E. Tatum**, **James Q. Chambers**, and **Zi-Ling Xue**[*]
Department of Chemistry, The University of Tennessee, Knoxville, TN 37996, USA

Abstract

A new, sensitive platform for the simultaneous electrochemical assay of Zn(II), Cd(II) and Pb(II) in aqueous solution has been developed. The platform is based on a new bimetallic Hg-Bi/single-walled carbon nanotubes (SWNTs) composite modified glassy carbon electrode (GCE), demonstrating remarkably improved performance for the anodic stripping assay of Zn(II), Cd(II) and Pb(II). The synergistic effect of Hg and Bi as well as the enlarged, activated surface and good electrical conductivity of SWNTs on GCE contribute to the enhanced activity of the proposed electrode. The analytical curves for Zn(II), Cd(II) an Pb(II) cover two linear ranges varying from 0.5 to 11 μg L^{-1} and 10 to 130 μg L^{-1} with correlation coefficients higher than 0.992. The limits of detection for Zn(II), Cd(II) are lower than 2 μg L^{-1} (S/N = 3). For Pb(II), moreover, there is another lower, linear range from 5 to 1100 ng L^{-1} with a coefficient of 0.987 and a detection limit of 0.12 ng L^{-1}. By using the standard addition method, Zn(II), Cd(II) and Pb(II) ions in river samples were successfully determined. These results suggest that the proposed method can be applied as a simple, efficient alternative for the simultaneous monitoring of heavy metals in water samples. In addition, this method demonstrates the powerful application of carbon nanotubes in electrochemical analysis of heavy metals.

Keywords

Anodic stripping voltammetry; Bimetallic film; Heavy metals; Single-walled carbon nanotubes; Bismuth

1. Introduction

Heavy elements such as zinc, cadmium and lead are an important group of pollutants that have been selected as the target for many stripping electroanalytical sensing methodologies at trace and ultratrace levels [1,2]. Because of the increased industrial use of the metals and their serious environmental impact, the development of new sensitive methods for quantifying trace amounts of these metals is required and challenged. These metal ions frequently coexist in many environmental samples with potential danger to aquatic life, especially at high levels. In recent years, the determination of potentially toxic metal ions in environmental samples has been a common concern, and there is growing need for simultaneous determination of toxic metals [3]. Nowadays, different techniques are used for

[*] Corresponding author. Phone: 001-865-974-3443; xue@ion.chem.utk.edu.

the simultaneous analysis [4-8]. Atomic absorption spectrometry techniques are accepted as a standard technique for metal determination, as they offers satisfactory sensitivity and fairly low acquisition cost [4]. However, the techniques usually measure only one element at a time. Inductively coupled plasma optical emission spectrometry (ICP-OES), on the other hand, offers multi-element analysis [5], but this technique is not yet extensively used in underdeveloped countries due to their high implementation and maintenance costs.

Electroanalytical methods offer advantages in analysis of metal ions such as high sensitivity, selectivity, simultaneous determination, simplicity and relatively low cost [9]. Among them, electrochemical stripping voltammetry (SV) is the most favorable because it comprises a variety of electrochemical approaches. It has an effective pre-concentration step and advanced electrochemical measurements of the accumulated analytes at/in the surface of the working electrode, allowing quantification of heavy metal ions often at ppb or even ppt levels [10-13].

Anodic stripping voltammetry (ASV) is the most popular stripping voltammetric method in trace and multielement analysis for heavy metals [14-17]. For the success of the stripping operation, the choice of the working electrode is crucial [18]. A great variety of electrode materials have been reported, such as gold, platinum, silver, mercury, iridium, several alloys, amalgams and antimony, etc [19-25]. Mercury-based electrodes have been mostly used for ASV due to superior electroanalytical performance of mercury over other candidates, despite its toxicity, and difficulties associated with its handling, storage, and disposal [10,26].

Recently, bismuth-based electrodes have been introduced as a favorable replacement for mercury electrodes and widely accepted in numerous electrochemical laboratories. Several configurations have been developed, including in situ, and ex situ bismuth film electrode (BiFE) [6,8], bismuth bulk electrode (BiBE) [7,27], bismuth powder modified carbon paste electrode (Bi-CPE) [28], and a Bi_2O_3 modified carbon paste electrode [29]. These electrodes possess behavior similar to the mercury electrode. However, there are limitations with Bi electrodes such as comparably high detection limits in some cases and additional polishing step of the carbon surface [30,31]. Current work prepared a bimetallic Hg-Bi film for the first time, which combines the advantages from both mercury and bismuth to improve the performance of the electrode, especially for stripping analysis.

Carbon nanotubes (CNTs) have been shown to possess potential for heavy metal analysis due to their strong sorption properties, high electrical conductivity, high surface area, significant mechanical strength, and good chemical stability [32]. The presence of CNTs on the electrode surface enhances the electrochemical activity of the electrode. In the current work, single-walled carbon nanotubes (SWNTs) are combined with bimetallic Hg-Bi to make Hg-Bi/SWNTs composite on a glassy carbon electrode. Studies show that such a new Hg-Bi/SWNTs composite modified electrode offers remarkably improved voltammetric behavior for stripping measurements of Zn(II), Cd(II) and Pb(II) in aqueous solution and in a river water sample. To our best knowledge, this is the first report on the preparation of the bimetallic Hg-Bi film and the application of such a bimetallic Hg-Bi/SWNTs composite electrode in the simultaneous determination of the metals in river samples.

2. Experimental

2.1. Apparatus and chemicals

All voltammetric measurements were preformed using a modulated potentiostat (CHI 650a, CH Instruments, Inc). A three-electrode configuration consisted of a Hg-Bi/SWNTs modified glassy carbon electrode, Ag/AgCl, and a platinum wire (CH Instruments, Inc) as

working, reference and counter electrodes, respectively. Acetic acid (HAc, glacial, 99.9%, Fisher), sodium acetate (NaAc, anhydrous, Certified ACS, Sigma-Aldrich), potassium chloride (KCl, 100%, Mallinckrodt), cadmium acetate (Cd_2Ac-3H_2O, Certified ACS, Fisher), and lead nitrate ($Pb(NO_3)_2$, Certified ACS, Fisher) were used as received. Hg(II), Bi(III) and Zn(II) AA standard solution (1000 mg L^{-1}, Aldrich) were diluted prior to use. SWNTs (<2 nm diameter) were purchased from Shenzhen Nanotech Port Ltd. Co. (China). The buffer solution (pH 6.0) contained 0.1 M KCl and 0.1 M NaAc/HAc. The buffer solution (pH 4.5) was prepared by mixing 0.1 M NaAc and 0.1 M HAc. Pb(II), Cd(II), and Zn(II) standards with different concentrations were prepared by diluting the appropriate amount of stock solution in electrolytes. All aqueous solutions were prepared in ultrapure water (>18 MΩ).

SWNTs of a certain mass were dispersed in 30% HNO_3 and then refluxed for 24 h at 140 °C to obtain carboxylic group-functionalized SWNTs. The resulting suspension was centrifuged, and the sediment was washed with deionized water until the pH reached 7.0. Then, the oxidized SWNTs were dispersed in deionized water to a concentration of 0.5 mg mL^{-1}.

2.2. Electrode modification with Hg-Bi/SWNTs

A glassy carbon electrode (GCE, 3 mm diameter, CH Inc) was polished to a mirror like surface using a standard electrode polishing kit (CH Instruments) including a 1200 grit Carbimet disk, 1.0 and 0.3 μm alumina slurry on a nylon cloth, and 0.05 mm alumina slurry on a microcloth polishing pad. After successive sonication in deionized water, ethanol (95%, Decon Laborataries, Inc, USA), and deionized water, 3.2 μL of 0.5 mg mL^{-1} caroxylic group-functionalized SWNTs solution was dropped on the pretreated GCE and dried in N_2 flow. Before the formation of Hg-Bi film, the SWNTs-coated GCE was then immersed in 0.1 M NaAc/HAc (pH 4.5) solution containing 100 mg L^{-1} of a mixture of Hg and Bi (4:1) ions for 4 min under stirring. Right after that, the ex-situ codeposition of Hg and Bi was performed at -1.0 V for 2 min under stirring. After carefully rinsing with deionized water, the obtained Hg-Bi/SWNTs/GCE was used for subsequent assays, and the electrode was used for many times. The process is simpler than the common, in-situ Bi or Hg film deposition, which has to be removed and redeposited after each detection [33].

2.3. Sample preparation

River samples were collected in polypropylene bottles from the Emory River, in Harriman, Tennessee, USA, and obtained shortly after the contamination from a massive coal fly ash spill [34]. Prior to analysis, the river samples from three locations of the river were mixed and acidified by 3% nitric acid. Afterwards, the samples were filtered and stored in a freezer and the sample was diluted before use. 0.1 M acetate buffer solution (pH 6.0) was prepared with the pretreated river water and used as river samples for the determination of Zn(II), Cd(II) and Pb(II), where the pH was then adjusted to 6.0 with a KOH (86.6%, Fisher, USA) solution. Standard additions of Zn(II), Cd(II) and Pb(II) were added, individually, to the river water, to a total volume of 20 mL. Zn(II) additions ranged from 0 to 12 μg L^{-1}, Cd(II) from 0 to 2 μg L^{-1} and Pb(II) from 0 to 5 μg L^{-1}.

2.4. Analytical procedure

For ASV experiments, 20 mL of standard solutions were used without deaeration. Convective accumulation of Zn (II), Cd(II) and Pb(II) on the Hg-Bi/SWNTs/GCE was carried out at a deposition potential of -1.3 V under stirring for 5 min. After the accumulation time, the anodic voltammetric measurements were registered in the quiescent solution by square wave voltammetry (SWV) with frequency of 15 Hz, step potential of 4 mV and amplitude of 25 mV. The potential sweep was ended at -0.3 V (vs Ag/AgCl). The

SWV scan started immediately upon completion of the accumulation time. No resting period was used between the accumulation and stripping steps. Stirring at high speed was required during the accumulation process but was stopped at the end of the quiet period for the stripping step. Between measurements, an electrochemical pre-cleaning step was applied in 0.1 M NaAc/HAc solution containing 0.1 M KCl at -0.3 V for 60 s, to guarantee the efficient removal of Zn (II), Cd (II) and Pb (II).

3. Results and discussion

3.1. Electrochemical characterization and surface morphological study of different electrodes

Fig. 1 shows the impedance measurements for bare GCE as well as GCE modified with Hg-Bi, Hg/SWNTs, Bi/SWNTs and the bimetallic Hg-Bi/SWNTs composites, respectively. The bare GCE showed the highest impedance, and the Hg-Bi coating on the surface of GCE decreased the impedance, demonstrating a favorable coating for electron transfer over bare GCE. The presence of SWNTs greatly improved the electron transfer of the electrode, leading to much lower impedances, indicating the good conductivity of SWNTs. The stripping signal of the electrode towards the metals of interest may be enhanced due to improvement in electron transfer on the modified electrode surface (Fig. 2A). No obvious difference was found among the electrodes modified with Bi/SWNTs, Hg/SWNTs and Hg-Bi/SWNTs composites. At this stage, the surface morphology of the electrode plays a primary role in the detection of analytes. Fig. S1 displays the surface morphologies of electrodes modified with Hg-Bi (Fig. S1a), Bi/SWNTs (Fig. S1b), Hg-SWNTs (Fig. S1c) and Hg-Bi/SWNTs (Fig. S1d). The Hg-Bi film was not stable on the bare GCE surface, and easily came off the electrode surface. Bi/SWNTs/GCE showed the coarsest surface, which may affect the performance of the electrode. In comparison, the bimetallic Hg-Bi/SWNTs/GCE displayed a uniform and smooth surface, and was thus favorable for the stripping detection of Zn(II), Cd(II) and Pb(II). The bimetallic Hg-Bi/SWNTs/GCE was subsequently used for simultaneous stripping detection of Zn(II), Cd(II) and Pb(II).

3.2. Electrochemical behavior of Zn(II), Cd(II) and Pb(II) at bimetallic Hg-Bi/SWNTs/GCE

The anodic stripping voltammetric technique is known to be one of the most sensitive techniques in the electroanalysis of trace metals. It involves two steps for the detection of Zn(II), Cd(II) and Pb(II): (i) accumulation of three metals at an optimized potential for a certain duration of time and (ii) anodic stripping of accumulated three metals. The anodic stripping signal has been used to monitor the concentration of Zn(II), Cd(II) and Pb(II) in solution. Fig. 2B shows the anodic stripping peaks of Zn(II) at -1.08 V, Cd(II) at -0.68 V and Pb(II) at -0.52 V in a 0.1 M pH 6.0 NaAc/HAc solution containing 0.1 M KCl at different electrodes examined in this work. The bare GCE did not show good peak shapes for three metals. The bimetallic Hg-Bi/GCE (Fig. 2Bc) exhibited the enhanced stripping peaks for Zn(II), Cd (II) and Pb (II) due to the conductive coating on the electrode surface. In the presence of SWNTs, the ASV behaviors of Bi/SWNTs/GCE, Hg/SWNTs and Hg-Bi/SWNTs/GCE are compared in Fig. 2Bb, d and e An obvious negative peak potential shift and wide peak shape at Bi/SWNTs/GCE were observed with slightly higher response to three metals than that obtained by bare GCE (Fig. 2Ba). In the presence of SWNTs, the improvement in stripping peak signals of Zn(II), Cd (II) and Pb (II) were observed at both the Hg (Fig. 2Bd) and Hg-Bi film (Fig. 2Be) coated GCE. However, best the stripping peak currents of Zn(II), Cd (II) and Pb (II) were observed at bimetallic Hg-Bi/SWNTs/GCE, suggesting a synergistic effect of Hg-Bi/SWNTs composite. The composite provides an advantageous and high-performance platform for the sensing of Zn(II), Cd (II) and Pb (II). These results agreed well with the impedance results and surface morphologies of the electrodes discussed earlier.

3.3. Optimization of experimental conditions

In order to obtain the best voltammetric behavior of the bimetallic Hg-Bi/SWNTs composite electrode towards Zn(II), Cd(II) and Pb(II), several parameters including KCl concentration, the mass ratio of Hg to Bi, the concentration of Hg and Bi, the amount of SWNTs, the quiet time before codeposition of Hg and Bi, the deposition potential and time and the preconcentration time of Zn(II), Cd(II) and Pb(II) were examined in detail (Fig. 3).

3.3.1. Effect of KCl concentration—The KCl concentration plays an important role in the electron transfer on the electrode surface, and was thus first optimized. As shown in Fig. 3A, the peak currents of three metals increased with the increasing KCl concentration, which could be explained by the increasing electron transfer speed resulting from the increasing ionic strength. No obvious change in the peak current was observed, when KCl concentration was higher than 0.1 M, so the 0.1 M KCl was chosen as the optimal for the subsequent assay.

3.3.2. Effect of the mass ratio of Hg to Bi—The mass ratio of Hg and Bi in the bimetallic film has a large impact on the contribution of the synergistic effect of the two metals to the enhanced activity of Hg-Bi/SWNTs composite electrode. Fig. 3B shows the difference in detection behavior of Hg-Bi/SWNTs composite electrode prepared with the different ratio of Hg to Bi. The increasing ratio increased the peak currents of Zn (II), Cd(II) and Pb(II). The highest response was observed at Hg /Bi ratio of 4:1. Further increase in the ratio made the response of the composite electrode decrease As mentioned in Fig. 2, Hg-Bi/SWNTs composite electrode showed higher response than either Hg/SWNTs or Bi/SWNTs electrode, indicating the synergistic effect contributed to the improved behavior of the proposed electrode for the detection of Zn (II), Cd(II) and Pb(II). Moreover, low content of Bi in the bimetallic film could improve the electrode performance, but higher Bi content had negative effect on the performance for the metal detection. The Hg/Bi ratio of 4:1 was used as the optimal one for the subsequent assay.

3.3.3. The concentration of Hg and Bi ions and the SWNTs amount—Both the concentration of Hg(II)/Bi(III) ions and the amount of SWNTs have profound effect on the electrochemical response of the Hg-Bi/SWNTs/GCE. The concentration of Hg(II)/Bi(III) ions controlled the thickness of the bimetallic film. As shown in Fig. 3C, the peak heights of Zn(II), Cd(II) and Pb(II) displayed a clear dependence on the bimetallic Hg/Bi film thickness as they increased with increasing concentrations of Hg(II)/Bi(III) ions from 1.0 to 250 mg L^{-1} However, for Hg/Bi concentrations higher than 100 mg L^{-1}, the stripping peak current of Zn(II) slightly decreased, but no obvious decrease in peak currents of Cd(II) and Pb(II) was found. Therefore, the optimized concentration of Hg/Bi was chosen as 100 mg L^{-1}.

The presence of SWNTs with enlarged, activated surface and good electrical conductivity on GCE also contributes to the enhanced activity of the Hg-Bi/SWNTs composite electrode (Fig. 3D). It was found the increasing SWNTs amount dramatically increased the peak currents of Zn(II), Cd(II) and Pb(II), which was because the crease in SWNTs amount enlarged the electrode surface and enhanced the electron transfer on the electrode surface. When the amount was more than 3.2 μL, no obvious change in the peak currents was found, due to the saturation of active sites on the electrode surface. In comparison with the reports in literature [2], this proposed method offered an additional unique advantage of using Hg-Bi/SWNTs composite electrode in that providing the electrode with higher sensitivity for Zn(II), Cd(II) and Pb(II) detection.

3.3.4. Quiet time before codeposition of Hg and Bi—Under the deposition pH of 4.5, which is near to the pKas of most carboxylic acids, the electrostatic interaction will occur between the negatively charged carboxylic group-functionalized SWNT and the Hg(II) and Bi(III) ions in the deposition solution. So setting a quiet time before the codeposition of Hg and Bi was favorable for the good distribution of Hg and Bi ions on the surface of SWNTs, which is helpful for the formation of good surface morphology of Hg-Bi film. As shown in Fig. 3E, longer quiet time could give rise to a higher peak current, which is because longer quiet time could lead to a good distribution of Hg and Bi ions on the surface of SWNTs, resulting in the formation of a high-quality Hg-Bi film. The highest peak currents for Zn(II) and Pb(II) were found when the quiet time was 300 s, while a quiet time of 240 s was found to give the highest peak current for Cd(II). Considering the lowest response of the proposed electrode towards Cd(II), 240 s was used as the optimal quiet time for the codeposition of Hg and Bi.

3.3.5. Deposition potential and time of Hg and Bi—Effects of the deposition potential and time of Hg and Bi on the surface of SWNTs/GCE on the Zn(II), Cd(II) and Pb(II) stripping responses were also investigated. From -0.9 to -1.1V, the effect of the deposition potential on the stripping signal was explored (Fig. 3F). The best stripping signal was obtained at -1.0 V. A more negative or positive deposition potential than -1.0 V was found to decrease the stripping signal of the target metals. This might be assigned to the incomplete reduction of Hg and Bi at a more positive potential and the reduction of hydrogen at a more negative potential, which may weaken the stripping behavior of the Hg-Bi/SWNTs composite electrode towards Zn(II), Cd(II) and Pb(II) by affecting surface morphology of Hg/Bi film.

The relationship between the stripping signal of the three metals and the deposition time of Hg and Bi at -1.0 V on SWNTs/GCE was also studied (Fig. S2). The peak currents increased proportionally with time between 30 and 120 s. The curves went down at deposition time longer than 120 s. This was probably because a longer deposition time would increase the thickness of the Hg-Bi film. Therefore, the deposition potential and time of -1.0 V and 120 s were used for the following assays.

3.3.5. Preconcentration time of Zn (II), Cd(II) and Pb(II) before stripping—The preconcentration of Zn (II), Cd(II) and Pb(II) was carried out under the potential of -1.3 V. The effect of the preconcentration time in the range from 60 to 420 s was studied (Fig. S3). The increase of the peak current was in proportion to the increasing preconcentration time between 60 to 300 s. It may be attributed to the enhanced accumulation of the metals on the electrode surface. The curve was found to level off for the three metals when the preconcentration time was longer than 300 s, indicating a saturation of the available electrode surface sites for the deposition of Zn(II), Cd(II) and Pb(II). It is supposed that no more metals ions can be deposited once the three metals cover the entire Hg-Bi/SWNTs/ GCE surface.

4. Analytical performance for the detection of Zn(II), Cd(II) and Pb(II)

Under the optimized chemical and electrochemical variables, the Hg-Bi/SWNTs/GCE was applied for the simultaneous determination of Zn(II), Cd(II) and Pb(II) by SWASV. The SWASV results for different concentrations of Zn(II), Cd(II) and Pb(II) in 0.1 M acetate solution containing 0.1 M KCl were illustrated in Figs. 4, 5 and 6. The analytical curves for all three metals covered two linear ranges varying from 0.5 to 11 μg L^{-1} and 10 to 130 μg L^{-1} with correlation coefficients higher than 0.992. In the concentration range from 0.5 to 11 μg L^{-1} (Fig. 4a and b), the calibration plot was well linear up to 11 μg L^{-1} for all three metals, and the detection of limits (LOD) of 0.23 μg L^{-1} for Zn (II), 0.076 μg L^{-1} for Cd(II),

and 0.18 μg L^{-1} for Pb(II) were obtained based on a signal-to-noise ratio equal to 3 (S/N = 3). In the concentration range from 10 to 130 μg L^{-1} (Fig. 5a and b), the good linear calibration plot was also found up to 130 μg L^{-1} for all three metals with LODs of 2 μg L^{-1} for Zn(II), 0.98 μg L^{-1} for Cd(II) and 1.3 0.98 μg L^{-1} for Pb(II). Moreover, a lower linear range of Pb(II) from 5 to 1100 ng L^{-1} was achieved with a coefficient of 0.987 and a LOD of 0.12 ng L^{-1} (Fig. 6a and b). Such a high sensitivity and low LOD obtained is most likely ascribed to the synergistic effect of Hg-Bi/SWNTs composite. Table 1 summarizes the calibration curves, the correlation coefficients and LODs of the tree analyte ions, indicating that the bimetallic Hg-Bi/SWNTs constructs a high-performance platform for the sensing of Zn(II), Cd(II) and Pb(II). Our results demonstrate that the proposed Hg-Bi/SWNTs composite is reliable for the detection of all three metals at ppb, even ppt level, which is expected to be used for real samples analysis.

5. Interference studies

In the SWASV determination of Zn(II), Cd(II) and Pb(II), interferences may come from the codeposition of foreign ions, occupying the active sites supposed to be for analyte ions on the electrode surface. Thus foreign ions were tested to evaluate the possible interference with the simultaneous detection of 10 μg L^{-1} Zn(II), Cd(II) and Pb(II) in the 500-fold mass ratio of interferent to analyte under the optimized method (Table 2). For this task, the peak current decrease was used for the interference investigation. The results indicated that Ru(III) and Rh(III) showed the obvious influences on the signals of Zn(II), Cd(II) and Pb(II). The foreign ion was considered as interferent when it caused a change at ca. 10% in regards to the response of the analyte signal alone. As verified, the interference was observed for the signal of Zn(II). No obvious interferences were found for the detection of Cd(II) and Pb(II) by the other foreign ions. The interferences possibly came from two aspects: competition between analytes and interferent ions for the sites of the Hg-Bi/SWNTs composite and intermetallic compound formation. Despite the interference, for practical analysis, applying standard addition method in simultaneous determination of Zn(II), Cd(II) and Pb(II) eliminated the interferences as demonstrated by a successful analysis of a contaminated river water discussed below.

6. Analysis of river water samples

To further demonstrate the practicality of the present electrode, it was evaluated by the application in the simultaneous determination of Zn(II), Cd(II) and Pb(II) in contaminated river samples using standard addition method (Table 3). The stripping signals of Zn(II), Cd(II) and Pb(II) were all observed with Hg-Bi/SWNTs/GCE. The original concentrations of Zn(II), Cd(II) and Pb(II) in the river samples were tested to be 15.9±1.4 μg L^{-1}, 1.51±0.48 μg L^{-1}, and 5.55±0.65 μg L^{-1}, respectively, which were confirmed by means of comparison with the data from ICP-OES. A difference of 7.4% for Zn(II), 11.8% for Cd(II), and 0.5% for Pb(II) and good recoveries (higher than 98.2%) were obtained, indicating that the proposed method was highly accurate, precise and reproducible. It can be used for direct analysis of relevant real samples.

7. Conclusions

In this work, a high-performance and sensitive platform for the stripping analysis of Zn(II), Cd(II) and Pb(II) has been successfully built. This platform is based on a bimetallic Hg-Bi/SWNTs composite. Bimetallic Hg/Bi is homogenously distributed in the surface of SWNTs forming a smooth and uniform film. The preparation and optimization of a bimetallic Hg-Bi/SWNTs composite are well studied. Such a composite film greatly facilitates the electron-transfer processes and the sensing behavior for Zn(II), Cd(II) and Pb(II) detection, leading to

a remarkably improved stripping behavior over either mercury- or bismuth film-based electrodes. The resulting chemical sensor exhibits good applicability for the detection of Zn(II), Cd(II) and Pb(II) in contaminated river samples collected from Emory River, Harriman, Tennessee, USA.

Supplementary Material

Refer to Web version on PubMed Central for supplementary material.

Acknowledgments

References

1. Tarley CRT, Santos VS, Baeta BEL, Pereira AC, Kubota LT, Hazard J. Mater. 2009; 169:256–262.
2. Injang U, Noyrod P, Siangproh W, Dungchai W, Motomizu S, Chailapakul O. Anal Chem Acta. 2010; 668:54–60.
3. Li YQ, Hu JM, Yang JG, Zheng B, Ha YQ. Anal Chim Acta. 2002; 461:181–188.
4. Tarley CRT, Arruda MAZ. Anal Sci. 2004; 20:961–966. [PubMed: 15228119]
5. Becka NG, Franks RP, Bruland KW. Anal Chim Acta. 2002; 455:11–22.
6. Wang J, Lu JM, Hocevar SB, Farias PAM, Ogorevc B. Anal Chem. 2000; 72:3218–3222. [PubMed: 10939390]
7. Armstrong KC, Tatum CE, Dansby-Sparks RN, Chambers JQ, Xue ZL. Talanta. 2010; 82:675–680. [PubMed: 20602953]
8. Hocevar SB, Daniele S, Bragato C, Ogorevc B. Electrochim Acta. 2007; 53:555–560.
9. Cobelo-Garcia A, Prego AP. Anal Chim Acta. 2004; 524:109–114.
10. Wang J. Electroanalysis. 2005; 17:1341–1346.
12. Economou A. Trends Anal Chem. 2005; 24:334–340.
13. Wang, J. Analytical electrochemistry. 3rd. John Wiley & Sons; Hoboken, New Jersey, USA: 2006.
14. Pilkington ES, Weeks C, Bond AM. Anal Chem. 1976; 48:1665–1669.
15. Bultstein H, Bond AM. Anal Chem. 1976; 48:759–761.
16. Vos L, Komy Z, Reggers G, Roekens E, Van Grieken R. Anal Chim Acta. 1986; 184:271–280.
17. Aldstadt JH, Dewald HD. Anal Chem. 1992; 64:3176–3179.
18. Wang J, Deo RP, Thongngamdee S, Ogorevc B. Electroanalysis. 2001; 13:1153–1156.
19. Achterberg EP, Braungardt C. Anal Chim Acta. 1999; 400:381–397.
20. Wang J, Tian B. Anal Chem. 1993; 65:1529–1532. [PubMed: 8328670]
21. Nolan MA, Kounaves SP. Anal Chem. 1999; 71:3567–3573.
22. Wang J, Hocevar SB, Deo RP, Ogorevc B. Electrochem Commun. 2001; 3:352–356.
23. Mikkelsen Ø, Schrøer KH. Electroanalysis. 2001; 13:687–692.
24. Fischer J, Barek J, Yosypchuk B, Navratil T. Electroanalysis. 2006; 18:127–130.
25. Tesarova E, Baldrianova L, Hocevar SB, Svancara I, Vytras K, Ogorevc B. Electrochim Acta. 2009; 54:1506–1510.
26. Economou A, Fielden PR. Talanta. 1998; 46:1137–1146. [PubMed: 18967239]
27. Pauliukaite R, Hocevar SB, Ogorevc B, Wang J. Electroanalysis. 2004; 16:719–723.
28. Hocevar SB, Svancara I, Vytras K, Ogorevc B. Electrochim Acta. 2005; 51:706–710.
29. Krolicka A, Pauliukaite R, Svancara I, Metelka R, Bobrowski A, Norkus E, Kalcher K, Vytras K. Electrochem Commun. 2002; 4:193–196.
30. Korolczuk M, Moroziewicz A, Grabarczyk M. Anal Bioanal Chem. 2005; 382:1678–1682. [PubMed: 16021422]

31. Pan D, Wang Y, Chen ZP, Lou TT, Qin W. Anal Chem. 2009; 81:5088–5095. [PubMed: 19435334]

32. Trojanowicz M. Trends Anal Chem. 2006; 25:480–489.

33. Rico MAG, Olivares-Marin M, Gil EP. Electroanalysis. 2008; 24:2608–2613.

34. Surface Water Sampling Results, Kingston Fossil Fly Ash Response January 10th 2009, Revision 1, Technical Direction Document TTEMI-05-001-0084. U.S. Environmental Protection Agency; 2009.
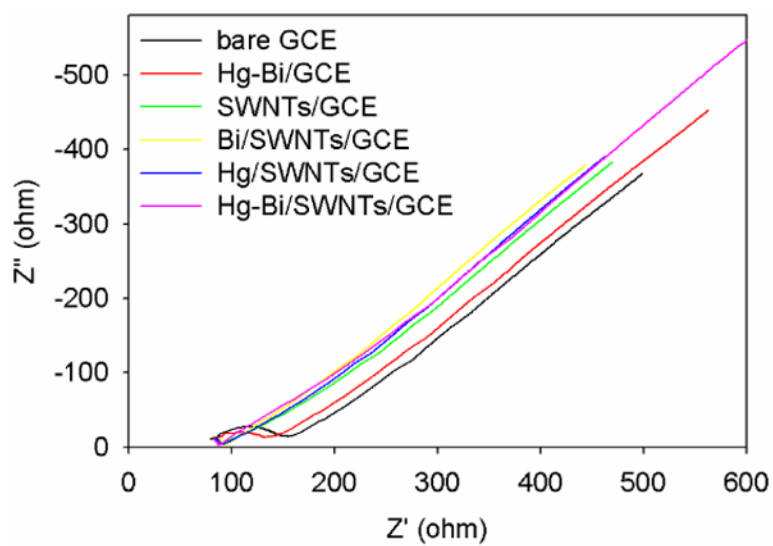
Fig. 1.
Impedances measurements of 5 mM $[Fe(CN)_6]^{3-/4-}$ at bare GCE, Hg-Bi/GCE, Bi/SWNTs/ GCE, Hg/SWNTs/GCE and Hg-Bi/SWNTs/GCE in 0.1 M KCl.
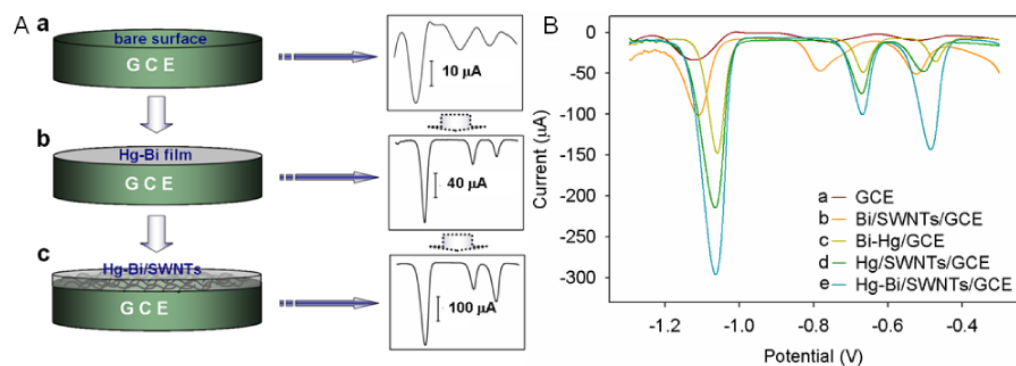
Fig. 2.
(A) Schematic illustration of the detection behaviors of bare GCE (a), Hg-Bi/GCE (b) and Hg-Bi/SWNTs/GCE (c) towards Zn (II), Cd(II) and Pb(II). (B)Voltammetric behaviors of a) bare GCE, b) Bi/SWNTS/GCE, c) Hg-Bi/GCE, d) Hg/SWNTs/GCE and e) Hg-Bi/SWNTs/ GCE towards 100 μg L^{-1} Zn (II), Cd(II) and Pb(II) in 0.1 M NaAc/HAc containing 0.1 M KCl (pH 6.0).
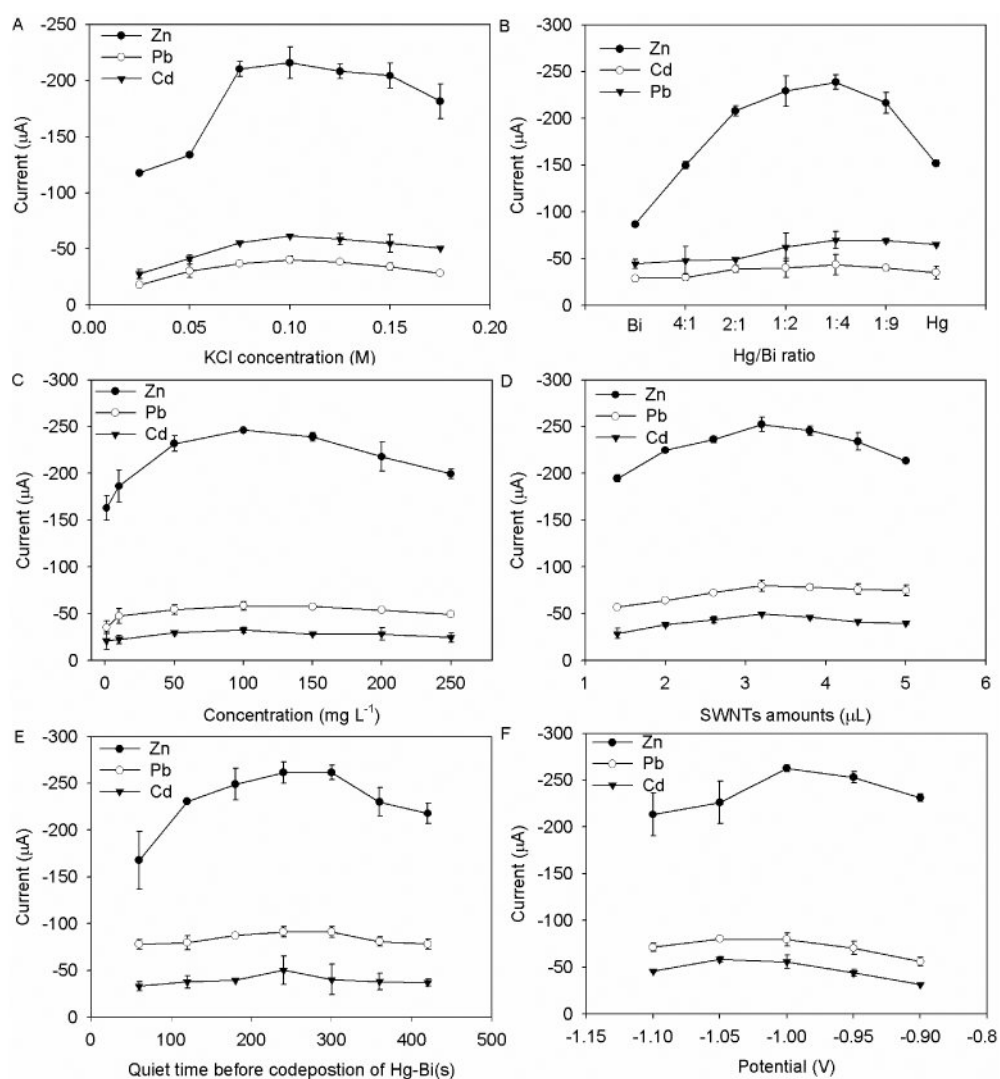
Fig. 3.
Effect of (A) KCl concentration, (B)the mass ratio of Hg to Bi, (C) Hg/Bi concentration, (D) quiet time before codeposition of Hg and Bi, (E) quiet time before codeposition of Hg and Bi, and (F) the deposition potential of Hg and Bi on the stripping signal of 100 μg L^{-1} Zn (II), Cd(II) and Pb(II) in 0.1 M NaAc/HAc (pH 6.0). The experimental parameters for (A) are Hg:Bi ratio: 2:1, Hg/Bi concentration: 50 mg L^{-1}, SWNTs amount: 2.0 μL, quiet time before Hg/Bi deposition: 120 s, deposition potential: -1.1 V, Hg/Bi deposition time: 60 s, preconcentration time: 240 s. The followings used the optimized parameters obtained. Error bar: n = 3.
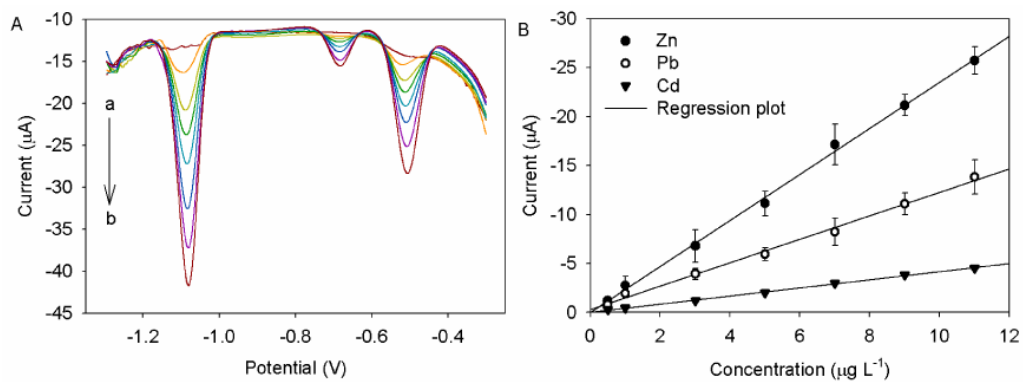
Fig. 4.
(A) Stripping performance and (B) the corresponding calibration plots of Hg-Bi/SWNTs/ GCE towards Zn (II), Cd(II) and Pb(II) at different concentrations (from a to h: 0.5, 1, 3, 5, 7, 9, and 11 μg L^{-1}, respectively). Error bar: n = 3.
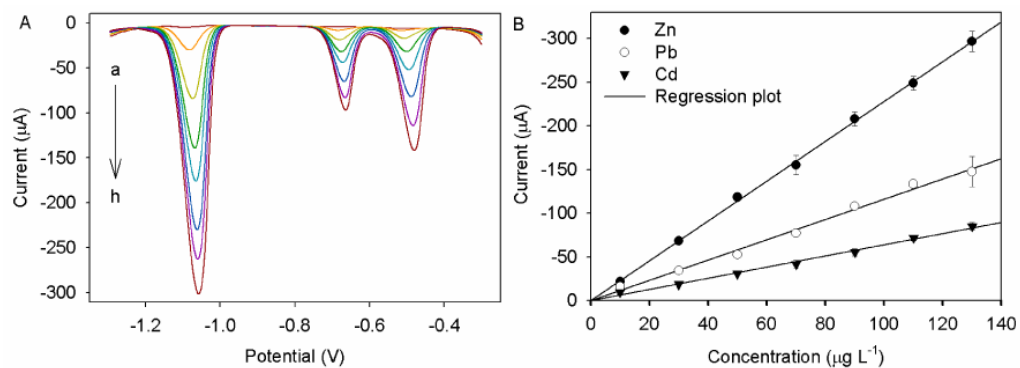
Fig. 5.
(A) Stripping performance and (B) the corresponding calibration plots of Hg-Bi/SWNTs/ GCE towards Zn (II), Cd(II) and Pb(II) at different concentrations (from a to h: 0, 10, 30, 50, 70, 90, 110, and 130 μg L^{-1}, respectively). Error bar: n = 3.
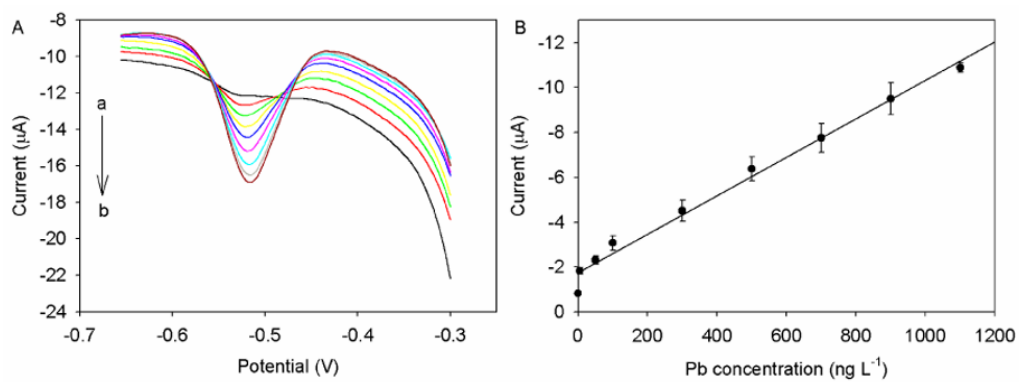
Fig. 6.
(A) Stripping performance and (B) the corresponding calibration plots of Hg-Bi/SWNTs/
GCE towards Pb(II) at different concentrations (from a to i: 0, 5, 50, 100, 300, 500, 700,
900, and 1100 ng L^{-1}, respectively). Error bar: n = 3.

Table 1

Summary of calibration curves, the correlation coefficients and LODs of Zn(II), Cd(II) and Pb(II) at Hg-Bi/SWNTs/GCE.

Concentration range	Ions	Calibration curve	R^2	LOD ($\mu g\ L^{-1}$)
	Zn(II)	y = -2.28 × - 0.15	0.999 ± 0.005	2.0 ± 0.07
10~130 $\mu g\ L^{-1}$	Cd(II)	y = -0.64 × - 0.03	0.992 ± 0.004	0.98 ± 0.02
	Pb(II)	y = -1.16 × - 0.03	0.992 ± 0.004	1.3 ± 0.09
	Zn(II)	y = -2.35 × - 0.04	0.998 ± 0.002	0.23 ± 0.004
0.5~11 $\mu g\ L^{-1}$	Cd(II)	y = -0.41 × - 0.03	0.995 ± 0.001	0.076 ± 0.002
	Pb(II)	y = -1.15 × - 0.90	0.999 ± 0.006	0.18 ± 0.006
5~1100 $ng\ L^{-1}$	Pb(II)	y = -8.57 × - 1.75	0.987 ± 0.003	0.12 ($ng\ L^{-1}$) ± 0.005

Note: y and x refer to the peak current and concentration of the anayte metal, respectively.

Error bar: n = 3

Table 2

Interference study of Zn(II), Cd(II) and Pb(II) determination.

Foreign ions	Peak current decrease (%)			Foreign ions	Peak current decrease (%)		
	Pb (II)	Zn (II)	Cd (II)		Pb (II)	Zn (II)	Cd (II)
Cu^{2+}	1.68%	22.4%	7%	Cr^{3+}	11.8%	23.2%	15.5%
Al^{3+}	10.6%	13%	-14.5%	$PtCl_6^{2-}$	4.89%	20.9%	-46.5%
Ni^{2+}	-7.6%	19.8%	19.1%	In (III)	12%	16.2%	-15.1%
MoO_4^{2-}	7%	21.9%	-23.9%	Rh (III)	23.1%	73.2%	100%
Fe^{3+}	8.8%	16.8%	-10%	Ru (III)	8.26%	89.7%	89.4%
Sn^{2+}	-9.46%	17.4%	-1.67%	Sr^{2+}	-21.9%	16.6%	-9.05%
SeO_4^{2-}	0%	12.4%	-1.83%	VO_4^{3-}	10.6%	24.3%	8.9%
AsO_4^{3-}	10.5%	22.1%	-15.5%	BrO_3^-	3.1%	9.5%	10.2%
Pd^{2+}	9.5%	18%	20.1%	ClO_4^-	7.8%	19.4%	10.6%
Ta (V)	11.4%	19.5%	-37.5%	CrO_4^{2-}	7.72%	15.7%	-9.6%

Note: The mass ratio of interferant to analyte is 500:1.

Table 3

Determination of Zn(II), Cd(II) and Pb(II) in the contaminated river water.

Sample	Added (μg L⁻¹)			Found by ICP-OES (μg L⁻¹)			Found by proposed method (μg L⁻¹)			Recovery(%)		
	Zn(II)	Cd(II)	Pb(II)	Zn(II)	Cd(II)	Pb(II)	Zn(II)	Cd(II)	Pb(II)	Zn(II)	Cd(II)	Pb(II)
River water	–	–	–	14.8±0.92	1.18±0.13	5.58±0.55	15.9±1.36	1.32±0.48	5.55±0.65	–	–	–
	6	0.5	1	–	–	–	6.00±0.38	0.49±0.09	1.01±0.15	100	97.9	101
	9	1	3	–	–	–	8.97±0.82	1.04±0.34	2.88±0.31	99.7	104	98.2
	12	2	5	–	–	–	12.25±1.21	2.03±0.17	4.89±0.42	102.2	101.5	99.6

Note: The determination was carried out three times. Error bar: n = 3